Progress In Electromagnetics Research C, Vol. 129, 231–243, 2023

Design and Analysis of a 4-Port MIMO Microstrip Patch Antenna for 5G Mid Band Applications

Suman Sharma* and Mukesh Kumar

Abstract—This article proposes a 4-port MIMO antenna for 5G mid-band application resonating from 4.5–5.1 GHz which comes under n79 band, an FR1 5G NR band used in smart phones. The first design involves a single-element microstrip patch antenna with a diamond shaped slots and partial ground structure of size $30 \times 43 \times 1.6\,\text{mm}^3$. Using this single element antenna as reference, a 4 port MIMO antenna is presented which operates at 4.9 GHz resonance frequency with proper spacing, resulting in much improved isolation between the elements. The proposed 4 port MIMO antenna is designed and fabricated over a commercially available low-cost FR-4 substrate having a relative dielectric permittivity of 4.4 and thickness of 1.6 mm. The $W \times L$ dimension of this MIMO antenna is $56 \times 56\,\text{mm}^2$. Simulation of the S-parameters and radiation pattern of all purposed designs is performed using the CST studio suite, and test results of the return loss are presented using the Keysight N9916A 14 GHz vector network analyzer. Antenna gain is 3.8 dB, and efficiency is 87% with a low (less than 0.1) envelope correlation coefficient (ECC) between any two radiating elements, paired with a positive diversity gain (DG), indicating that the proposed antenna is well designed. As a result, the proposed antenna is an excellent candidate for deployment in 5G networks.

1. INTRODUCTION

In order to achieve the growing requirements of the network, wireless communication and fifth generation (5G) are developing rapidly. A significant increase in throughput is expected from 5G, especially for LTE (long-term evolution) [1]. Extensive use of communications requires high data rates, low latency, and massive connectivity for vehicle communications, transportation, environmental monitoring, and smart cities [2, 3]. There are two bands in the 5G network, mmWave band and sub-6 GHz band [4, 5]. Sub-6 GHz describes mid frequency radio bands below 6 GHz, while mmWave describes higher frequency radio bands between 24 GHz and 40 GHz. Low-frequency bands are below 1 GHz [6]. There is enormous potential for standardization in the higher 5G band. Sub-6 GHz, on the other hand, is considered to be a more realistic standard that will be more widely deployed [7, 8]. Compared to low-band, 5G mid-band offers faster speeds and more capacity, and along with this, it offers a significantly broader coverage area. Compared to high-band millimetre wave (mmWave) spectrum, mid-band spectrum, unlike mmWave, may pass through walls. In highly populated urban regions where connectivity demand is high, 5G mid-band provides a balance of speed, capacity, coverage, and penetration that is particularly remarkable [6]. In the sub-6 GHz band, five licensed 5G bands are allotted with n77 and n79 being the most industry oriented. The n79 band is an FR1 5G NR (New Radio) band. It uses the Time Division Duplexing (TDD) mode which only needs one frequency band for both uplink and downlink [9, 10]. In 5G communication, multiple-input multiple output (MIMO) and massive MIMO systems are used as the antennas to overcome path losses and atmospheric attenuations. Data rates and channel capacity increase with the increase in number of antenna elements in a MIMO system. However, the overall

Received 1 December 2022, Accepted 3 February 2023, Scheduled 8 February 2023
* Corresponding author: Suman Sharma (sumansharma@skit.ac.in).
The authors are with the Swami Keshvanand Institute of Technology Management & Gramothan, Jaipur, India.

system becomes complex when the number of elements increases, since the correlation increases. That is why low correlation and high isolation are the basic requirements for MIMO systems [11–16].

There have been several antennas proposed in papers [17–21] for 5G systems in both sub-6 GHz and mmWave which included n77, n79, LTE band 42, 43 MIMO systems and mmWave arrays. A triband MIMO antenna with eight elements is presented in [21], offering a low correlation characteristics. In [22], an eight-element MIMO antenna is described with both planar resonators. The hybrid assembly makes it difficult to fabricate the antenna system, even though the isolation between radiating elements is as good as 15 dB. In [23], a four-port MIMO dielectric resonator antenna (DRA) system with size $80 \times 80\,\text{mm}^2$ is described which provides spatial and diversity characteristics. In [24], a six-element MIMO antenna system of $136 \times 68\,\text{mm}^2$ is described that has a peak gain of 3.1 dB with low correlation among MIMO elements. [25] presents a 28 GHz, 4-port MIMO antenna array of size $30 \times 35\,\text{mm}^2$ with 8-elements and peak gain 3.6 dBi. It is demonstrated in [26] how a metasurface can increase the gain of a two-port circularly polarized WLAN band antenna. MmWave band with 4 GHz bandwidth is characterized by a two-port orthogonal MIMO configuration in [27]. A simple feeding mechanism presented in [28, 29] for four-element linearly polarized planar structures.

Here, in this paper, a 4-port MIMO antenna with diamond shaped slots into the patch and a defected ground structure is presented for 5G mid-band, resonating in n79 band which is used in 5G smart phone applications. The novelty of this work lies in the fact that the proposed antenna works in n79 band under the C band, which is widely used around the world but very small number of researches done for this band. n79 band is running across Australia, China, the European Union including UK, Hongkong, Japan, Isreal, New Zealand, the Philippines, Singapore, South Korea, and more. Apple iPhone 12 and iPhone 13 series as well as one plus 10 pro already have n79 band. So this antenna will prove to be a very good candidate for the mobile phones having 5G connectivity because of its compact size, efficiency, and good bandwidth factors. All four elements of the antenna are placed in such a way that it provides good isolation among all ports as well as a high gain and high efficiency.

The complete layout of the paper is as follows. An analysis of the literature review is presented in Section 1. Section 2 presents the geometry and simulation results of the proposed single element antenna, including S-parameter, radiation pattern, E-plane and H-plane plots, and the surface current. A four element MIMO antenna for sub-6 GHz 5G application is proposed, simulated, analyzed, and tested in Section 3. The summary of the results and a comparative study of this work with the other works reported in the references are shown in Section 4, and Section 5 concludes the complete work.

2. DESIGN PROCESS OF PROPOSED ANTENNA AND ITS CONFIGURATIONS

2.1. Single Element Antenna

The first step of the process is to design a single element antenna as shown in Fig. 1. The front side and back side of the design are shown in Figs. 1(a) and 1(b), respectively. The antenna is designed using a square patch radiator, connected with a $50\,\Omega$ microstrip feed line, a ground plane, and an FR4 substrates with relative dielectric permittivity of 4.4 and thickness of 1.6 mm. Diamond shaped slots are cut into the patch as square-, diamond-, and pentagon-shaped slots giving wide band response and perfect impedance matching, when being designed properly. The antenna is designed to resonate at frequency 4.9 GHz which comes under the n79 band of 5G mid-band spectrum. The single element antenna's design parameters are as follows: substrate width $Ws = 30$ mm, substrate length $Ls = 43$ mm, patch length $Lp = 11$ mm, patch width $Wp = 12$ mm, length of feed line $Lf = 2$ mm, width of feed line $Wf = 1.4$ mm, diameter of each diamond shaped slot $D_x = 4$ mm, dimensions of small rectangle slot in ground $= 2\,\text{mm} \times 5\,\text{mm}$, and dimensions of large rectangle slot in ground is $2\,\text{mm} \times 24\,\text{mm}$. Two strips are connected in ground plane to achieve a symmetric structure of MIMO antenna following the connected ground plane theory according to which complete ground plane used for MIMO antenna should be connected.

Figure 2 explains the complete design flow of the antenna from starting to final design, which helps to understand how the required results are achieved.

This single element antenna was designed using the CST studio suite, and its simulation results of reflection coefficients are measured using Keysight N9916A 14 GHz vector network analyzer. This single element antenna is used to further design a 4-element MIMO antenna explained later in Section 3.

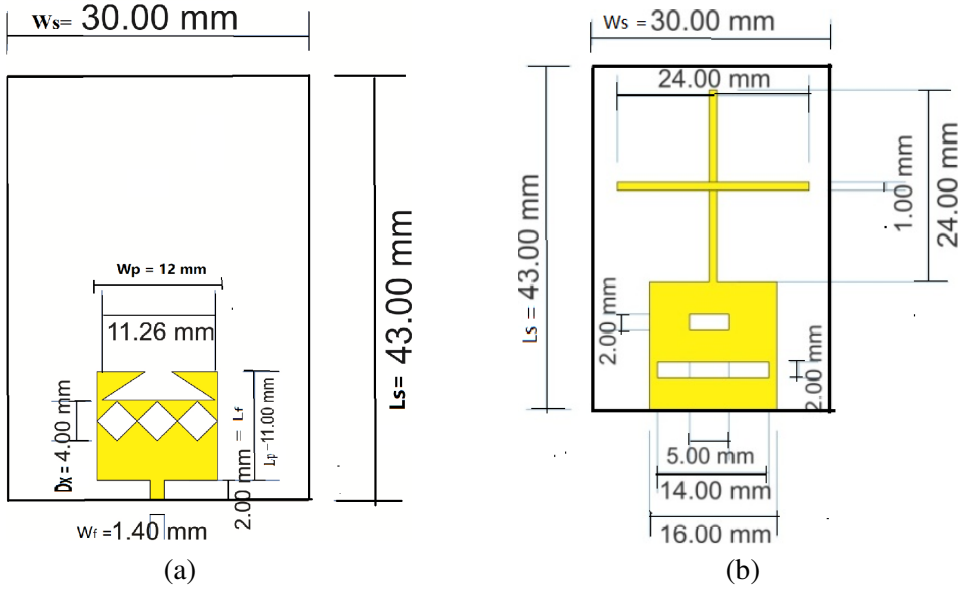

Figure 1. Single element antenna structure. (a) Front side, (b) back side.

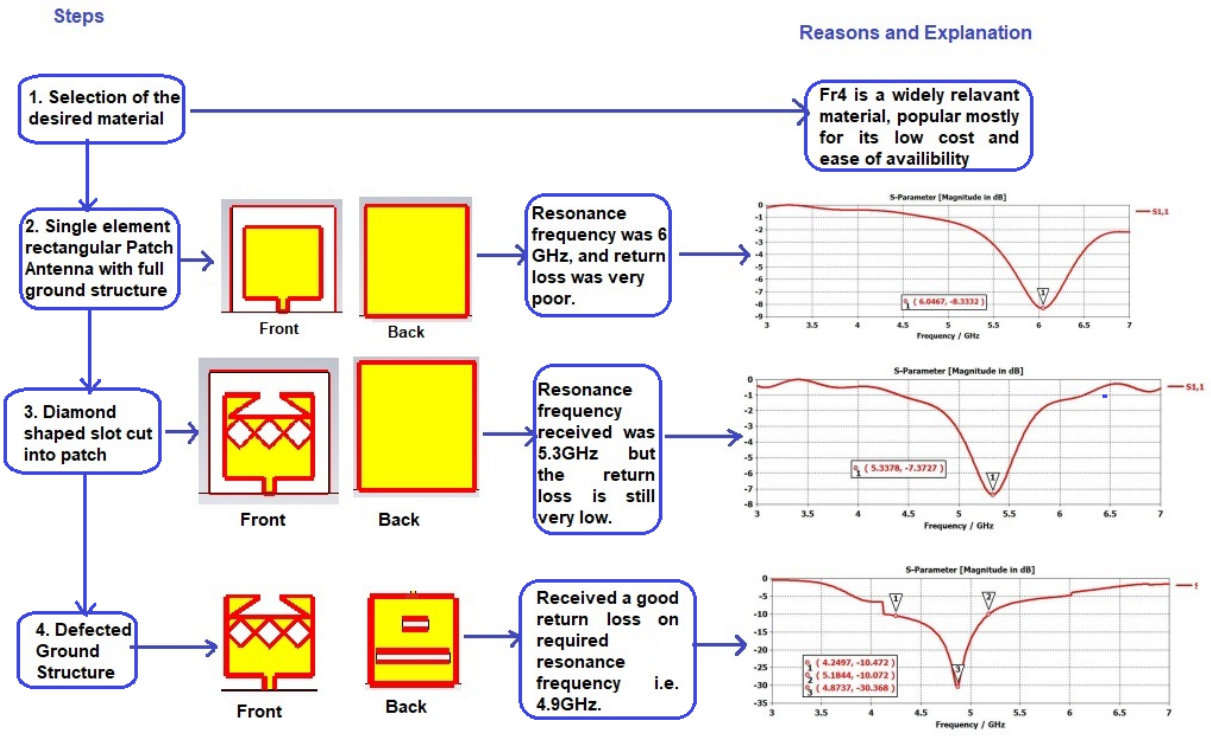

Figure 2. Complete design flow of the proposed antenna.

Simulation result of reflection coefficients is shown in Fig. 3(a) which depicts that S_{11} parameter is -33 dB at resonant frequency 4.9 GHz showing the minimum return loss and good impedance matching. The bandwidth of proposed single element antenna is 800 MHz which is sufficient for 5G mid-band communication. Fig. 3(b) shows gain and efficiency curves with respect to frequency. Maximum IEEE gain observed over frequency is 3.44 dB which can be further increased by using low dielectric loss

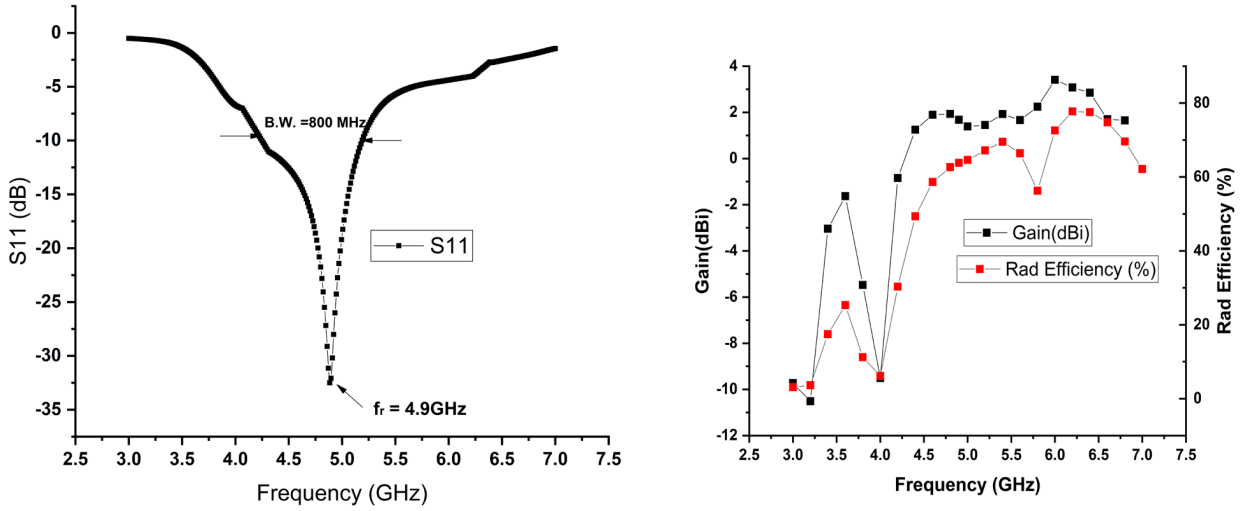

Figure 3. (a) Simulated graph for reflection coefficient. (b) Plot of maximum gain and radiation efficiency over frequency.

material like Rogers RT5880 substrate. Efficiency of the proposed antenna is 81% which makes it a good candidate for 5G smart phone applications.

The 3D radiation pattern and surface current distribution of a single element antenna are illustrated in Fig. 4. The distribution of surface current in Fig. 4(b) shows that most current flows along the surface of the patch as well as along the feed line.

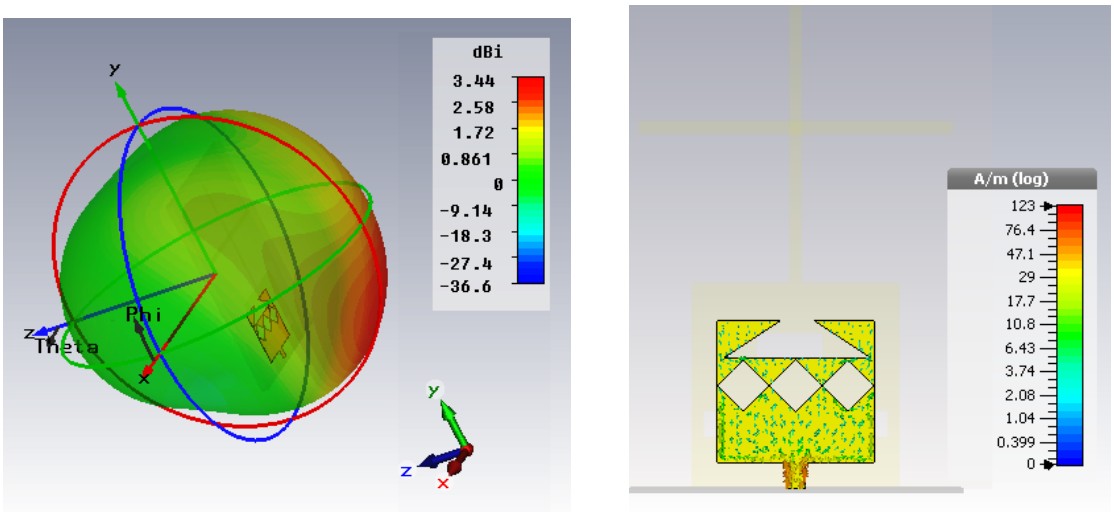

Figure 4. (a) 3D radiation pattern and (b) surface current distribution.

3. FOUR ELEMENTS MIMO ANTENNA

An antenna system with a MIMO structure has wide application in 5G infrastructure due to its ability to withstand fading and lossy environments and to deliver a variety of performance characteristics [30]. A similar configuration is reported for sub-6 GHz and mmWave [31, 32].

Using the single element antenna design proposed in Section 2 as a reference, the front side and back side of a four-element MIMO antenna structure are presented in Figs. 5(a) and (b). Antenna dimensions of the antenna are $56 \times 56 \times 1.6\,\text{mm}^3$ with four elements symmetrically arranged in 90-degree rotation with each other, which is intended to achieve greater than 20 dB isolation across all the four ports [33]. Before this square box arrangements, many more arrangements are also tried, but this arrangement is the best structured arrangement from the perspective of overall size of the antenna. Due to this structure and its compact size, this antenna can be easily fitted in smart phones. Figs. 5(c) and (d) depict the front view and back view of the fabricated prototype antenna for 4-port MIMO systems.

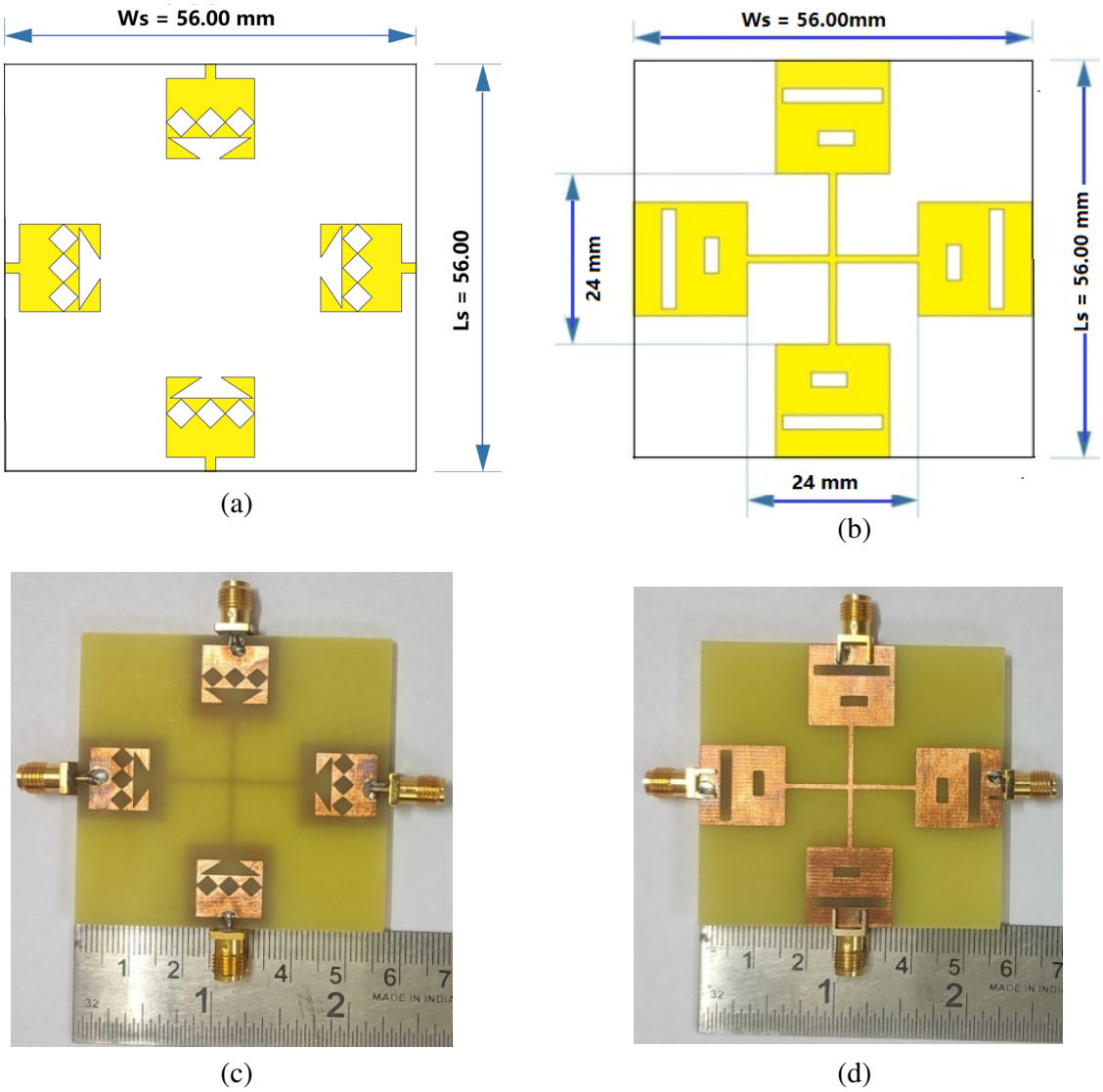

Figure 5. (a), (b) Proposed design of four port MIMO antenna and (c), (d) its fabricated prototype.

Due to multiple alike elements, there is high mutual interference and envelope correlation coefficient (ECC) between the various radiating elements. Consequently, it is hard to design a diversity antenna with four ports or more because the radiating elements interfere with each other. Therefore, the antenna structure is designed such that all four elements are on 90 degrees to each other placed on each of four sides of the substrate.

Upon simultaneous excitation of all four ports at 4.9 GHz, Fig. 6(a) depicts the surface current distribution in antenna. An electric current flowing in a conductor can be determined by observing

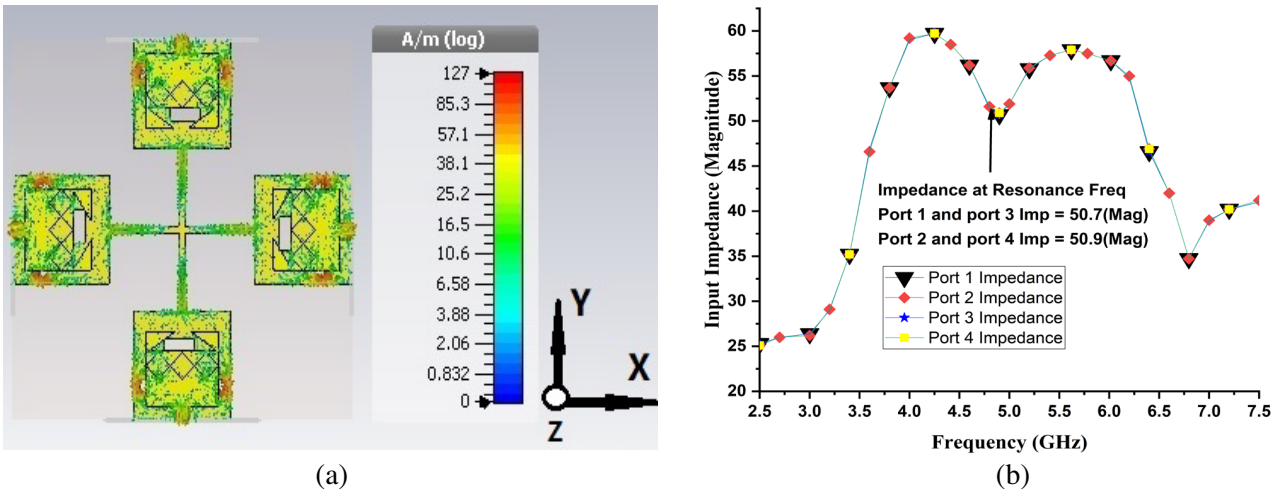

(a) (b)

Figure 6. (a) Distribution of surface current, (b) plot of input impedance at all four ports.

its surface currents. As suggested by [34], one port should be excited while the others should remain terminated with a 50 Ω load in order to understand the coupling effect between the antenna elements. Fig. 10 illustrates that maximum current flow is along the surface of the antenna elements, edges of the diamond slot, and around the feed line.

A plot of input impedance magnitude is shown in Fig. 6(b) which shows that there is a good impedance matching for all four ports of the MIMO antenna.

3.1. Proposed MIMO Antenna Results

This section presents an analysis of the simulated and test results. All the MIMO antenna elements are fed by 50 SMA (SubMiniature version A) end launch connectors. The performance of the antenna's far field radiation is tested in an anechoic chamber while the S-parameters are measured in open air using Keysight N9916A 14 GHz vector network analyzer. The prototype antenna is used as a receiver, and a well-calibrated conventional gain horn antenna is used as the broadcast antenna. The antenna is rotated during testing to measure the radiation intensity at various angles. By evaluating the diversity performance from the perspectives of the ECC, transmission coefficient, diversity gain, and mean effective gain, the proposed MIMO antenna system's reliability is verified.

3.1.1. S-Parameters Plot

Figure 7(a) shows the simulation and test results for the reflection coefficients S_{ii} for each of the four ports and it can be observed that both the results agree well. Only port 1 is excited when antenna element 1 is measured, and the other ports are terminated with a 50 load. The measurements for the remaining antenna elements are performed in a manner similar to this by excitation of the respective antenna port and connection of the 50 load to other ports. At resonance frequency 4.9 GHz, simulation results show that $S_{11} = S_{22} = S_{33} = S_{44} = -32$ dB, while test results show -23 dB for all four ports. S-parameters differ slightly in both simulated and test results, which can be due to the cable losses and measurement setup. The proposed MIMO antenna offers 800 MHz bandwidth which covers the 5G mid frequency band communication spectrum.

Mutual correlation between MIMO components can be observed using the transmission coefficient. Fig. 7(b) shows a plot of the simulated and measured transmission coefficients S_{ij} of the proposed MIMO antenna. When the proposed structure is used, the antennas have very low mutual coupling between the antenna elements. As shown in Fig. 7(b), there is less than -20 dB of mutual interference between MIMO antenna elements, in the whole operational bandwidth.

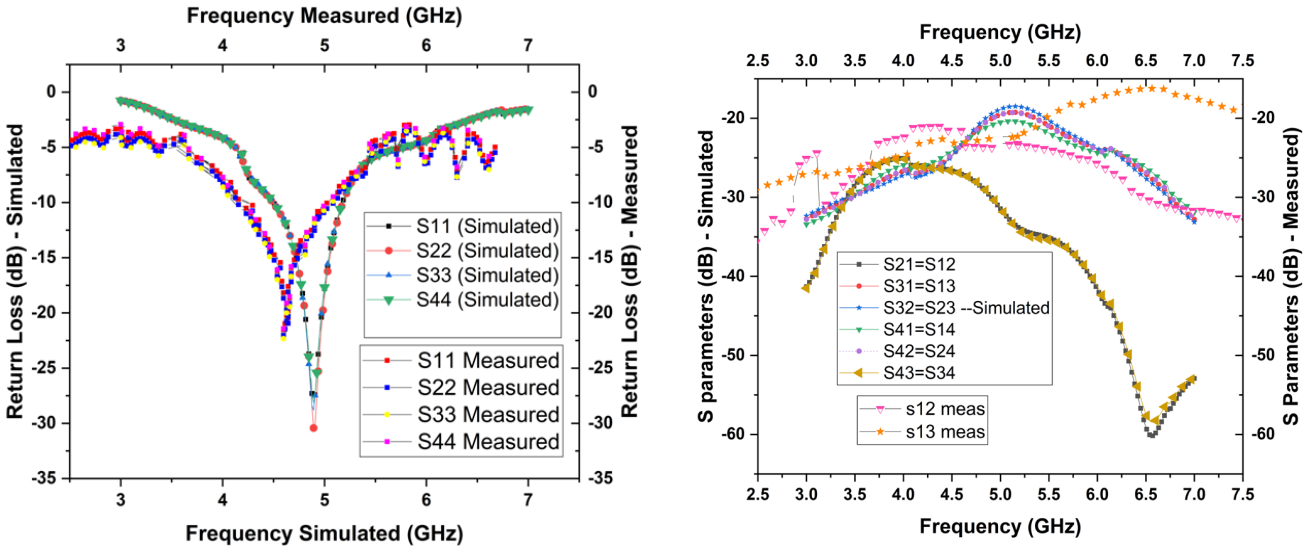

Figure 7. Simulation and test results of (a) reflection coefficients and (b) transmission coefficients.

3.1.2. Far Field Results

The aim of designing this MIMO antenna is to produce pattern diversity with a moderate gain value. 3D radiation pattern of proposed MIMO antenna is shown in Fig. 8(a), and it can be observed that 3D gain is 3.8 dBi at 4.9 GHz frequency which is higher than the single element antenna design. A measurement setup for far field measurement characteristics is shown in Fig. 8(b).

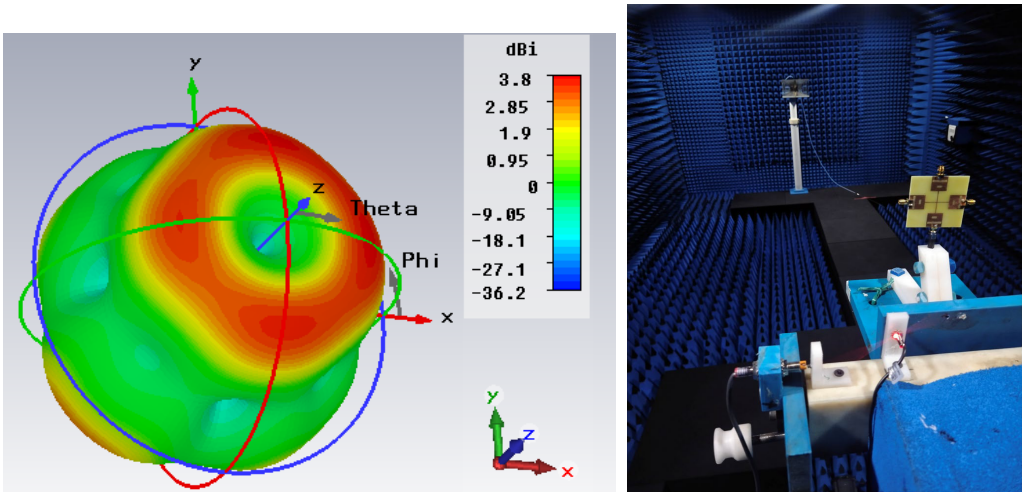

Figure 8. (a) Simulated 3D radiation pattern of proposed MIMO antenna, (b) photograph of far field measurement setup.

The simulated and measured results of radiation patterns for two principal planes, i.e., *E*-plane and *H*-plane are shown in Fig. 9 at 4.9 GHz frequency upon excitation of port 1. Results at all other ports are almost identical to the results upon exciting port 1. It can be observed that the directions of front lobe and back lobe are slightly away from the main axis (0 degrees and 180 degrees) in simulation

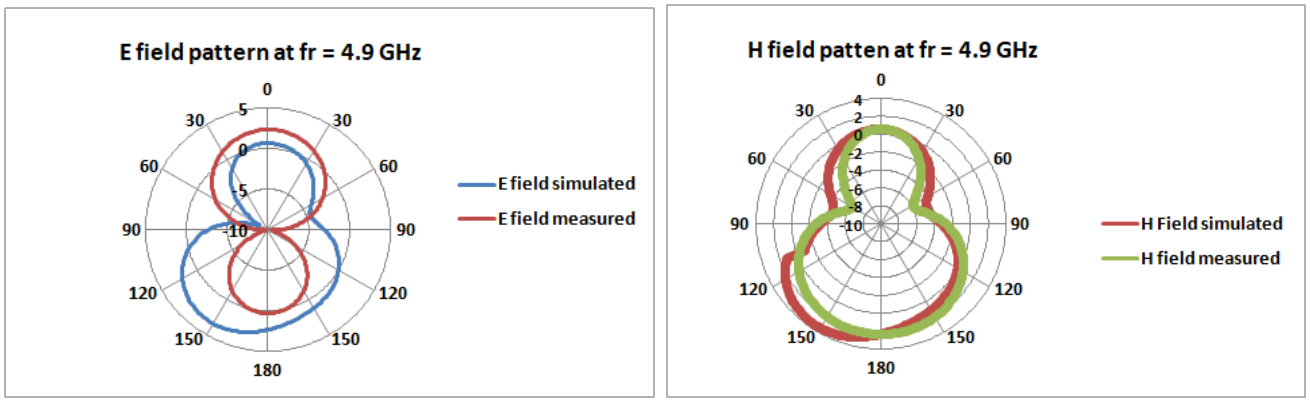

Figure 9. Simulated and measured E field and H field plots.

results, while in measured results the radiations are at 0 degree and 180 degree directions which make the antenna a good candidate for 5G communication. Negative front to back ratio may be further reduced by using reflector plates backside to the ground plane which will make this antenna more directional.

3.1.3. Gain and Radiation Efficiency

In order to analyze antenna performance, it is essential to know the antenna gain and efficiency. Proposed MIMO antenna's performance characteristics are discussed in this section. The antenna efficiency and gain curves (simulated and measured both) with respect to frequency are shown in Fig. 10, where the total efficiency varies from 80% to 90% for the entire bandwidth range, and the maximum gain is 3.8 dBi at the desired resonance.

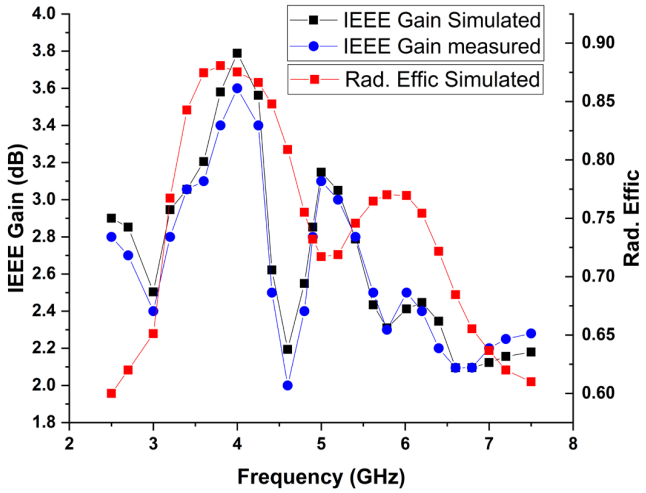

Figure 10. Plot of maximum gain and radiation efficiency over frequency.

3.1.4. Envelope Correlation Coefficient (ECC)

The performance independence of MIMO components, such as polarisation and radiation patterns, is measured by the ECC. The proposed MIMO antenna system's ECC is determined using Equation (1)

based on S-parameters and far-field radiation [35].

$$\mathrm{ECC} = \frac{\left|\iint 4\pi \left(\overrightarrow{A_i}(\theta,\varphi)\right) \xi \left(\overrightarrow{A_j}(\theta,\varphi)\right) \delta\omega\right|^2}{\iint 4\pi \left|\left(\left|\iint 4\pi \left(\overrightarrow{A_i}(\theta,\varphi)\right)\right|^2 \delta\omega\right)\left(\iint 4\pi \left(\overrightarrow{A_j}(\theta,\varphi)\right)\right)\right|^2 \delta\omega} \tag{1}$$

where $\overrightarrow{A_i}(\theta,\varphi)$ indicates the 3D far field pattern when port "i" is excited, and $\overrightarrow{A_j}(\theta,\varphi)$ indicates the 3D far field pattern when port "j" is excited. ω represents the solid angle. As shown in Fig. 11(a), the envelope correlation coefficient of the proposed antenna between any of the two antenna elements is less than 0.01, which indicates that they are very well correlated.

3.1.5. Diversity Gain (DG)

DG, which shows how the diversity scheme of MIMO antennas affects the radiated power, is another key parameter to measure performance of the MIMO antenna. Equation (2) is used to determine the DG for the proposed MIMO antenna based on the value of the S-parameters [35]. Because of the antenna's diversity gain, higher values result in better isolation. As shown in Fig. 11(a), a diversity gain of 9.99 dB is offered by the proposed MIMO antenna for each of its four antenna elements, which is close to the optimal value.

$$\mathrm{DG} = 10\sqrt{1 - (\mathrm{ECC})^2} \tag{2}$$

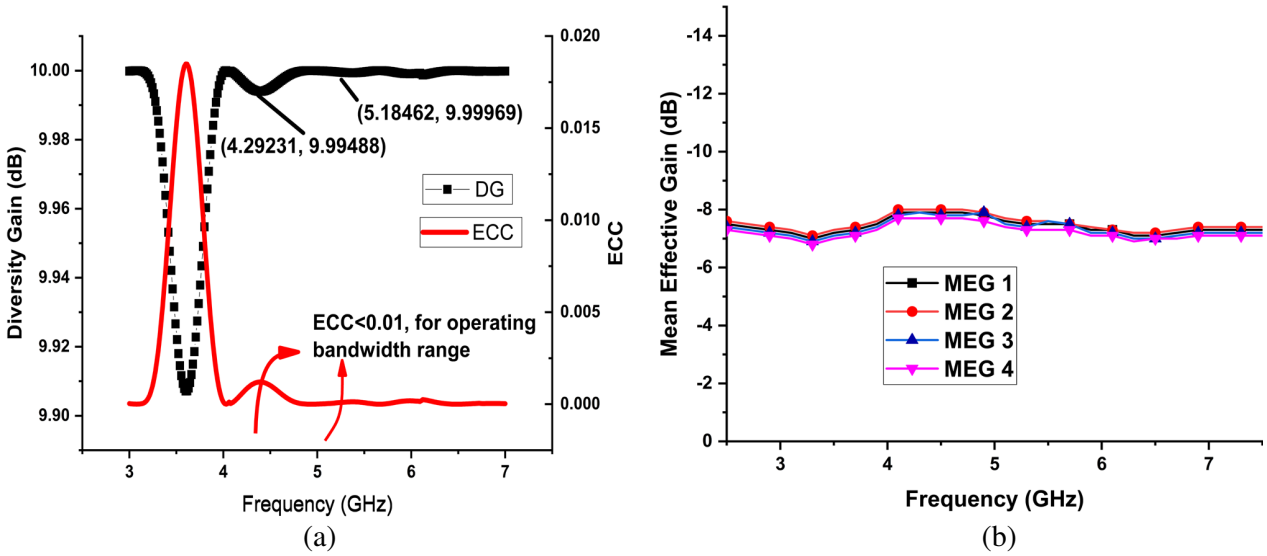

Figure 11. (a) DG and ECC plot of proposed MIMO antenna. (b) MEG plot.

3.1.6. Mean Effective Gain (MEG)

Another important parameter for measuring diversity performance of the MIMO antenna is MEG, which is a ratio of the mean received power to the mean incident power of the antenna [36]. The range of the practical MEG value that is acceptable should be between −3 dB and −12 dB [37]. Using Equation (3) the MEG value is calculated for the proposed antenna, and the value of MEG is in the range of identical values as shown in Fig. 11(b) [36, 37].

$$\mathrm{MEG}_i = 0.5\left(1 - \sum_{i=1}^{N} |S_{ij}|\right) \tag{3}$$

where i = port at which observations are taken and N = number of antenna elements in MIMO system.

4. COMPARATIVE ANALYSIS

The proposed MIMO antenna is compared with some of the antennas reported in the reference which is shown in Table 1. It can be noted that the proposed MIMO antenna has a number of advantages over the antennas discussed in literature, including its application that this n79 band is being used in many smart phones worldwide. Also, antenna size, number of radiating elements, gain, efficiency, and isolation between the antenna elements make it more efficient than other reported antennas.

Table 1. A comparative analysis of the proposed antenna with the antennas reported in literature.

Reference Paper	Freq. (GHz)	No. of antenna elements	Size ($L \times W$) in mm^2	Isolation between radiating elements (dB)	Peak Gain (dB)	Total Efficiency (%)	Envelope Correlation Coefficient	Minimum spacing between antenna elements
[15]	2.3–3.0/ 5.4–5.6	4	40×40	14	3.1	NA	< 0.2	8 mm
[18]	4.5–5.0	5	80×80	15	5.6	NA	< 0.01	NA
[19]	27–29	4	30×30	28	7	92	< 0.01	6 mm
[23]	3.3–3.8/ 5.5–5.5	4	80×80	18	4	70	< 0.2	28 mm
[28]	4.8–6.0	4	30×30	10	4.02	67	< 0.15	9 mm
[29]	5.15–5.35	4	112×112	22	4.8	89	< 0.15	NA
[34]	20–40	4	80×80	20	10	70	< 0.2	10.3 mm
[38]	27.5–29.5	4	30×30	26	5.8	90	< 0.03	3.4 mm
[39]	4.7–5.1	4	40×40	25	2.8	70	< 0.01	16 mm
Proposed	**4.5–5.1**	**4**	$\mathbf{56 \times 56}$	**20**	**3.8**	**87**	$\mathbf{< 0.01}$	**9 mm**

5. CONCLUSION

This paper presents a four port MIMO antenna with diamond shaped slots and a defected ground structure at 4.9 GHz frequency for 5G-n79 band using a correct impedance match. Antenna is designed and simulated on CST studio suite. The measurement of S-parameters is done using Keysight N9916A 14 GHz VNA, and far field results are measured using an anechoic measurement setup. This MIMO antenna is created using the proposed single element antenna, by putting all single elements 90 degrees apart from each other making a square form of structure. Overall diversity performance of the proposed MIMO antenna is very good as mutual coupling between antenna elements is less than -20 dB. Diversity gain is 10 dB, and ECC is less than 0.01, which are very near the ideal values. The proposed MIMO antenna is compact in size, i.e., $56 \times 56 \times 1.6$ mm^3 with operating bandwidth as 800 MHz, peak gain as 3.8 dBi with symmetrical and stable radiation pattern, and efficiency as 87% on resonance, making it a considerable viable candidate for 5G smart phone applications. Furthermore, the gain can be increased by using low dielectric loss material like RT/duroid 5880 or by increasing the number of antenna elements making an array form.

REFERENCES

1. Gheni, S. A. and D. K. Naji, "Optimal design of a circularly polarized antenna for LTE bands 42/43 applications," *Progress In Electromagnetics Research C*, Vol. 120, 223–241, 2022.
2. Gupta, A. and R. K. Jha, "A survey of 5G network: Architecture and emerging technologies," *IEEE Access*, Vol. 3, 1206–1232, 2015, doi: 10.1109/ACCESS.2015.2461602.

3. Arya, A. K., S. J. Kim, S. Park, D.-H. Kim, R. S. Hassan, K. Ko, and S. Kim, "Shark-fin antenna for railway communications in LTE-R, LTE, and lower 5G frequency bands," *Progress In Electromagnetics Research*, Vol. 167, 83–94, 2020.
4. Hussain, N., W. A. Awan, W. Ali, S. I. Naqvi, A. Zaidi, and T. T. Le, "Compact wideband patch antenna and its MIMO configuration for 28 GHz applications," *AEU — Int. J. Electron. Commun.*, Vol. 132, Apr. 2021, doi: 10.1016/j.aeue.2021.153612.
5. Anitha, R., P. V. Vinesh, K. C. Prakash, P. Mohanan, and K. Vasudevan, "A compact quad element slotted ground wideband antenna for MIMO applications," *IEEE Trans. Antennas Propag.*, Vol. 64, No. 10, 4550–4553, Oct. 2016, doi: 10.1109/TAP.2016.2593932.
6. Sufian, M. A., N. Hussain, H. Askari, S. G. Park, K. S. Shin, and N. Kim, "Isolation enhancement of a metasurface-based MIMO antenna using slots and shorting pins," *IEEE Access*, Vol. 9, 73533–73543, 2021, doi: 10.1109/ACCESS.2021.3079965.
7. Mohammed, S. L., M. H. Alsharif, S. K. Gharghan, I. Khan, and M. Albreem, "Robust hybrid beamforming scheme for millimeter-wave massive-MIMO 5G wireless networks," *Symmetry (Basel).*, Vol. 11, No. 11, 1424, Nov. 2019, doi: 10.3390/sym11111424.
8. Li, Z., Z. Du, M. Takahashi, K. Saito, and K. Ito, "Reducing mutual coupling of MIMO antennas with parasitic elements for mobile terminals," *IEEE Trans. Antennas Propag.*, Vol. 60, No. 2, 473–481, Feb. 2012, doi: 10.1109/TAP.2011.2173432.
9. Al-Bawri, S. S., M. T. Islam, M. J. Singh, et al., "Broadband sub-6 GHz slot-based MIMO antenna for 5G NR bands mobile applications," *Journal of Physics: Conference Series*, Vol. 1962, No. 1, Jul. 2021, doi: 10.1088/1742-6596/1962/1/012038.
10. Lalbakhsh, A., M. U. Afzal, K. P. Esselle, and S. L. Smith, "Wideband near-field correction of a Fabry-Perot resonator antenna," *IEEE Trans. Antennas Propag.*, Vol. 67, No. 3, 1975–1980, Mar. 2019, doi: 10.1109/TAP.2019.2891230.
11. Kamal, M. M., S. Yang, S. H. Kiani, et al., "Donut-shaped mmWave printed antenna array for 5G technology," *Electronics*, Vol. 10, No. 12, 1415, Jun. 2021, doi: 10.3390/electronics10121415.
12. Mohamadzade, B., R. M. Hashmi, R. B. V. B. Simorangkir, A. Lalbakhsh, and H. Ali, "A planar dynamic pattern-reconfigurable antenna," *2021 15th European Conference on Antennas and Propagation (EuCAP)*, 1–3, Mar. 2021, doi: 10.23919/EuCAP51087.2021.9411272.
13. Mohamadzade, B., R. B. V. B. Simorangkir, R. M. Hashmi, and A. Lalbakhsh, "A conformal ultrawideband antenna with monopole-like radiation patterns," *IEEE Trans. Antennas Propag.*, Vol. 68, No. 8, 6383–6388, Aug. 2020, doi: 10.1109/TAP.2020.2969744.
14. Sehrai, D. A., M. Asif, N. Shoaib, et al., "Compact quad-element high-isolation wideband MIMO antenna for mm-Wave applications," *Electronics*, Vol. 10, No. 11, 1300, Jun. 2021, doi: 10.3390/electronics10111300.
15. Sarkar, D. and K. V. Srivastava, "Compact four-element SRR-loaded dual-band MIMO antenna for WLAN/WiMAX/WiFi/4G-LTE and 5G applications," *Electron. Lett.*, Vol. 53, No. 25, 1623–1624, Dec. 2017, doi: 10.1049/el.2017.2825.
16. Elfergani, I., J. Rodriguez, A. Iqbal, M. Sajedin, C. Zebiri, and R. A. Abd Alhameed, "Compact millimeter-wave MIMO antenna for 5G applications," *2020 14th European Conference on Antennas and Propagation (EuCAP)*, 1–5, Mar. 2020, doi: 10.23919/EuCAP48036.2020.9136015.
17. Mohamadzade, B., R. B. V. B. Simorangkir, R. M. Hashmi, et al., "A conformal, dynamic pattern-reconfigurable antenna using conductive textile-polymer composite," *IEEE Trans. Antennas Propag.*, Vol. 69, No. 10, 6175–6184, Oct. 2021, doi: 10.1109/TAP.2021.3069422.
18. Jaiswal, R. K., K. Kumari, A. K. Ojha, and K. V. Srivastava, "Five-port MIMO antenna for n79-5G band with improved isolation by diversity and decoupling techniques," *Journal of Electromagnetic Waves and Applications*, Vol. 36, No. 4, 542–556, Mar. 2022, doi: 10.1080/09205071.2021.1975315.
19. Kamal, M. M., S. Yang, X.-C. Ren, et al., "Infinity shell shaped MIMO antenna array for mm-Wave 5G applications," *Electronics*, Vol. 10, No. 2, 165, Jan. 2021, doi: 10.3390/electronics10020165.
20. AboEl-Hassan, M., K. F. Hussein, and K. H. Awadalla, "A novel microstrip antenna with L-shaped slots for circularly polarized satellite applications," *Microw. Opt. Technol. Lett.*, Vol. 62, No. 2, 839–844, Feb. 2020, doi: 10.1002/mop.32083.

21. Zhao, A. and Z. Ren, "Wideband MIMO antenna systems based on coupled-loop antenna for 5G N77/N78/N79 applications in mobile terminals," *IEEE Access*, Vol. 7, 93761–93771, 2019, doi: 10.1109/ACCESS.2019.2913466.
22. Abdullah, M., S. H. Kiani, and A. Iqbal, "Eight element multiple-input multiple-output (MIMO) antenna for 5G mobile applications," *IEEE Access*, Vol. 7, 134488–134495, 2019, doi: 10.1109/ACCESS.2019.2941908.
23. Dwivedi, A. K., A. Sharma, A. K. Singh, and V. Singh, "Design of dual band four port circularly polarized MIMO DRA for WLAN/WiMAX applications," *Journal of Electromagnetic Waves and Applications*, Vol. 34, No. 15, 1990–2009, Oct. 2020, doi: 10.1080/09205071.2020.1801522.
24. Abdullah, M., S. H. Kiani, L. F. Abdulrazak, et al., "High-performance multiple-input multiple-output antenna system for 5G mobile terminals," *Electronics*, Vol. 8, No. 10, 1090, Sep. 2019, doi: 10.3390/electronics8101090.
25. Khalid, M., S. Iffat Naqvi, N. Hussain, M. Rahman, Fawad, S. S. Mirjavadi, M. J. Khan, and Y. Amin, "4-port MIMO antenna with defected ground structure for 5G millimeter wave," *Applications. Electronics*, Vol. 9, No. 1, 71, Jan. 2020, doi: 10.3390/electronics9010071.
26. Tran, H. H., N. Hussain, and T. T. Le, "Low-profile wideband circularly polarized MIMO antenna with polarization diversity for WLAN applications," *AEU — Int. J. Electron. Commun.*, Vol. 108, 172–180, Aug. 2019, doi: 10.1016/j.aeue.2019.06.028.
27. Zahra, H., W. A. Awan, W. A. E. Ali, N. Hussain, S. M. Abbas, and S. Mukhopadhyay, "A 28 GHz broadband helical inspired end-fire antenna and its MIMO configuration for 5G pattern diversity applications," *Electronics*, Vol. 10, No. 4, 405, Feb. 2021, doi: 10.3390/electronics10040405.
28. Yang, M. and J. Zhou, "A compact pattern diversity MIMO antenna with enhanced bandwidth and high-isolation characteristics for WLAN/5G/WiFi applications," *Microw. Opt. Technol. Lett.*, Vol. 62, No. 6, 2353–2364, Jun. 2020, doi: 10.1002/mop.32334.
29. Das, G., N. K. Sahu, A. Sharma, R. K. Gangwar, and M. S. Sharawi, "FSS-based spatially decoupled back-to-back four-port MIMO DRA with multidirectional pattern diversity," *IEEE Antennas Wirel. Propag. Lett.*, Vol. 18, No. 8, 1552–1556, Aug. 2019, doi: 10.1109/LAWP.2019.2922276.
30. Iqbal, A., A. Altaf, M. Abdullah, M. Alibakhshikenari, E. Limiti, and S. Kim, "Modified U-shaped resonator as decoupling structure in MIMO antenna," *Electronics*, Vol. 9, No. 8, 1321, Aug. 2020, doi: 10.3390/electronics9081321.
31. Kiani, S. H., A. Altaf, M. R. Anjum, etal., "MIMO antenna system for modern 5G handheld devices with healthcare and high rate delivery," *Sensors*, Vol. 21, No. 21, 7415, Nov. 2021, doi: 10.3390/s21217415.
32. Kiani, S. H., A. Altaf, M. Abdullah, et al., "Eight element side edged framed MIMO antenna array for future 5G smart phones," *Micromachines*, Vol. 11, No. 11, 956, Oct. 2020, doi: 10.3390/mi11110956.
33. Sharma, S. and M. Arora, "A millimeter wave elliptical slot circular patch MIMO antenna for future 5G mobile communication networks," *Progress In Electromagnetics Research M*, Vol. 110, 235–247, 2022.
34. Sehrai, D. A., M. Abdullah, A. Altaf, et al., "A novel high gain wideband MIMO antenna for 5G millimeter wave applications," *Electronics*, Vol. 9, No. 6, 1031, Jun. 2020, doi: 10.3390/electronics9061031.
35. Sufian, M. A., N. Hussain, A. Abbas, J. Lee, S. G. Park, and N. Kim, "Mutual coupling reduction of a circularly polarized MIMO antenna using parasitic elements and DGS for V2X communications," *IEEE Access*, Vol. 10, 56388–56400, 2022, doi: 10.1109/ACCESS.2022.3177886.
36. Kim, S.-H. and J.-Y. Chung, "Analysis of the envelope correlation coefficient of MIMO antennas connected with suspended lines," *J. Electromagn. Eng. Sci.*, Vol. 20, No. 2, 83–90, Apr. 2020, doi: 10.26866/jees.2020.20.2.83.
37. Tariq, S., S. I. Naqvi, N. Hussain, and Y. Amin, "A metasurface-based MIMO antenna for 5G millimeter-wave applications," *IEEE Access*, Vol. 9, 51805–51817, 2021, doi: 10.1109/ACCESS.2021.3069185.

38. Rahman, S., X.-C. Ren, A. Altaf, et al., "Nature inspired MIMO antenna system for future mmWave technologies," *Micromachines*, Vol. 11, No. 12, 1083, Dec. 2020, doi: 10.3390/mi11121083.
39. Ali, H., X.-C. Ren, I. Bari, et al., "Four-port MIMO antenna system for 5G n79 band RF devices," *Electronics*, Vol. 11, No. 1, 35, Jan. 2022, doi: 10.3390/electronics11010035.